Chemical Engineering Journal Advances 12 (2022) 100389

Contents lists available at ScienceDirect

Chemical Engineering Journal Advances

journal homepage: www.sciencedirect.com/journal/chemical-engineering-journal-advances

Magnetic coiffure: Engineering of human hair surfaces with polyelectrolyte-stabilised magnetite nanoparticles

Svetlana Konnova [a], Ramil Fakhrullin [a], Farida Akhatova [a], Nisha Lama [b], Yuri Lvov [b], Giuseppe Cavallaro [c], Giuseppe Lazzara [c], Rawil Fakhrullin [a,*]

[a] Institute of Fundamental Medicine and Biology Kazan Federal University, Kreml uramı 18, 420008,Kazan, Republic of Tatarstan, Russian Federation
[b] Institute for Micromanufacturing and Biomedical Engineering Program, Louisiana Tech University, 71272 Ruston, LA, United States of America
[c] Dipartimento di Fisica e Chimica, Università degli Studi di Palermo, Viale delle Scienze, pad. 17, 90128 Palermo, Italy

ARTICLE INFO

Keywords:
Hair surface engineering
Magnetic nanoparticles
Atomic force microscopy
Polyelectrolytes
Functionalisation

ABSTRACT

Here we report a spontaneous electrostatic coating of human hair with aqueous Fe_3O_4 colloids capable to tailor magnetic properties to hair, orienting and even moving them under the influence of the external magnetic field. Magnetite particles were modified by cationic and anionic polyelectrolytes and then successfully deposited in dense arrays, starting from cuticle gaps and spreading further over a major hair surface. These biocompatible and biodegradable magnetic nanoparticles may serve as carriers for drug loading and delivery for topical pharmaceutical treatments. The deposition process was imaged in real-time using dark-field microscopy. The hair specimens were further studied using a number of characterisation techniques. Under application of an external magnetic field, the nanoparticle magnetic ordering was obtained resulting in the hair alignment and attraction along the field applied. We believe the technology reported here will find a range of applications in topical drug delivery and hair care.

Introduction

Most of the mammals, including humans, are covered by hair, a filamentous protein (keratin) structure serving as means of skin protection from various environmental factors. In humans, hair plays a very important role as a functional and aesthetic part of the body. Beauty products have been developed to treat and modify the properties of the hair, including shampoos, conditioners, hair colorants and medicines. Healthy hair is among the most desired features, whereas the dissatisfaction with its colour, structure and density leads to various behaviour and psychological issues. In addition, hair is a versatile target for topical drugs applications. As a result, efforts have been focused at studies of human hair composition and structure and development of care formulations aimed at altering or modifying its properties [1–3]. Hair structure is quite conservative in all mammals; therefore, the treatments applicable for human hair modification can be successfully transferred to animal, including agricultural and pets.

Nanoarchitectonics approaches are highly promising for biomedical applications [4], including hair care products. We reported previously a hair surface engineering technique that is an architectonic deposition of nanoscale particles onto microcuticle scaled hair surface [5–7]. We demonstrated [8] that clay nanotubes are excellent candidates for topical drug deposition onto mammalian hair [8]. Self-assembly of nanoclays [9,10] stimulated us to investigate this phenomenon further and find out whether other nanoscale particles self-assemble on hair. In this study we focused on magnetic nanoparticles (MNPs). MNPs composed from the mixture of iron oxides are promising for imaging, magnetic fluid hyperthermia, separation of biomolecules, and targeted drug delivery for medical diagnosis and therapeutics [11,12]. They have sizes from few to hundred nanometers, are biocompatible and biodegradable, and can be used for tagging desired biological components as biomarkers; fluorescent MNPs were used for quick recognition of the targeted cells. Due to good penetrability of magnetic fields into human tissue, an external field gradient can be used to transport or immobilize MNPs with high precision at the particular organ's positions [11]. Low cargo loading performed by sorption, particularly for hydrophobic drugs, is one limitation, which may be overcome by using polymer–drug conjugates developing a layer-by-layer (LbL) coating of magnetic cores [13]. Elements of LbL self-assembly were also used for polyelectrolytes stabilization of magnetic nanoparticles. Anticancer drugs were

* Corresponding author.
E-mail address: kazanbio@gmail.com (R. Fakhrullin).

https://doi.org/10.1016/j.ceja.2022.100389

Available online 30 August 2022

immobilized on these nanoparticles for delivery to a targeted tumor regions reducing the risk of side effects and minimizing the dosage used in the treatment. MNPs introduced in body or blood stream can be heated in non-invasive manner with an high frequency oscillating magnetic field for chemo or radiotherapy enhancement treatment (hyperthermia) allowing for an effective destruction of malignant cells. These, in combination with MNPs biocompatibility, biodegradability and ease with which they can be tuned and functionalized have made them particularly interesting in oncological medicine with dual ability for targeted drug delivery accomplished with its marker control of their location [14].

Here we demonstrate the versatility of hair engineering expanding from clay nanotube hair coating to usage of magnetic nanoparticles. We have fabricated magnetic human hair by deposition of polyelectrolyte-stabilised iron oxide nanoparticles directly on human hair exploiting the nanoparticle concentration in the gaps of its cuticle organisation. Magnetite nanoparticles (MNPs) have been widely used with applications ranging from magnetic resonance imaging to directed drug delivery. Numerous studies reported tailoring various drugs to magnetic nanoparticles with the subsequent cellular internalisation.

Materials and methods

Chemicals

All chemicals used in this study were purchased from Sigma-Aldrich and used without further purification. Ultrapure water was obtained using a Millipore Simplicity water purification setup. Human hair samples were obtained from a female Caucasian volunteer. The hair was not stained or bleached before experiments.

Magnetic nanoparticles synthesis

Magnetic nanoparticles were synthesised via co-precipitation following our previously-published protocols [15,16]. Briefly, we prepared 2 M $FeCl_2 \bullet 4H_2O$ and 1 M $FeCl_3$ in 2 M aqueous HCl, which were mixed and heated while stirring to 75° C. Then, 1.5. M NaOH was added dropwise, which changed the suspension colour to dark, indicating the formation of iron oxide nanoparticles. The as-synthesised particles were separated from the supernatant and washed three times with water. For polyelectrolyte stabilisation, the pristine nanoparticles were suspended in aqueous 10 mg mL^{-1} solutions of either polyallylamine hydrochloride (PAH) or polystyrene sulfonate (PSS) (70 kDa), and sonicated for 20 min (4 × 5 min at 51% of maximal power) using a Bandelin Sonopuls GM 2070 sonifier. After that, the nanoparticles were incubated for 24 h on an orbital rotator, then collected via centrifugation and washed with water to remove the unbound polyelectrolytes.

Magnetisation of human hair

Hair samples (ca. 1 cm) were washed with water for 1 h, then immersed into aqueous suspensions of PAH or PSS-stabilised iron oxide nanoparticles. The following particles concentrations were tested: 1 mg mL^{-1}, 2 mg mL^{-1}, 3.1 mg mL^{-1}, 4.1 mg mL^{-1} and 5.1 mg mL^{-1}, whereas the exposure time originally was 1 h, then the following times: 5 min, 15 min, 30 min and 45 min were tested. The deposition was performed in 1.5 mL polymer test tubes placed onto a rotator. After the incubation, the hair samples were subjected to microscopy characterisation, as described below.

Transmission electron microscopy (TEM)

TEM images were obtained using a Hitachi HT7700 Exalens instrument. The as-synthesised MNPs suspended in water were dropped (ca 10 μL) onto carbon-coated lacey 3 mm copper grids and dried at room temperature. TEM images were collected at 100 kV accelerating voltage.

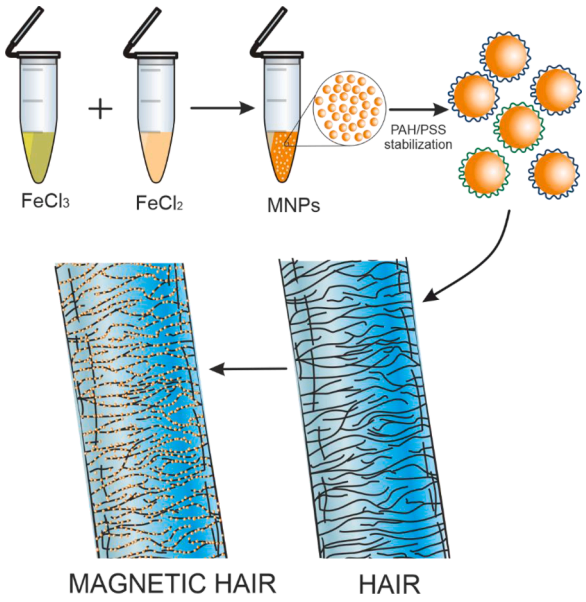

Fig. 1. A sketch demonstrating the strategy of human hair surface engineering using polyelectrolyte-stabilised magnetic nanoparticles deposited predominantly along the cuticle gap lines.

Zeta-potential (ZP) and dynamic light scattering (DLS) measurements

ZP and DLS measurements were performed using a Zetasizer Nano-ZS (Malvern) instrument in isothermal conditions (at 25 °C), the samples were placed into disposable folded capillary cells. During measurements, the laser wavelength and the scattering angle were 632.8 nm and 173°, respectively.

UV–vis spectrometry

Optical absorbance spectra and sedimentation real-time monitoring were performed using an Implen NanoPhotometer C80. The specimens (1 mL) were placed into tightly-closed quartz cuvettes and measured at 25 °C. For sedimentation monitoring, the optical density measurements were recorded during 5 h, with 10 s interval between measurement.

3D measurement laser scanning confocal microscopy

A confocal Olympus LEXT OLS5000 microscope (equipped with 100 × Olympus long working distance fluorite objective) was used to investigate the hair morphology and surface texture. Hair segments were tailored to glass slides using an adhesive type and imaged at ambient conditions in laser intensity and optical reconstruction modes. Laser and optical images were processed using OLS50-S-AA (Olympus) software media kit.

Atomic force microscopy (AFM)

Atomic force microscopy (AFM) imaging was performed following our previous protocol [6,8] using a Dimension Icon microscope (Bruker) and ScanAsyst-Air (Bruker) probes (tip radius 2 nm, nominal length 115 μm, spring constant 0.4 n m^{-1}). Raw data obtained in PeakForce Tapping QNM mode were processed using Nanoscope Analysis software v 3.0 (Bruker). AFM imaging was applied to pristine iron oxide nanoparticles to determine their shape and size distribution, and to image hair samples, which were positioned onto class slides, similarly to laser scanning confocal microscopy sample preparation. Strictly the top areas along the shaft of the hair were imaged using AFM to minimise the effects of surface curvature.

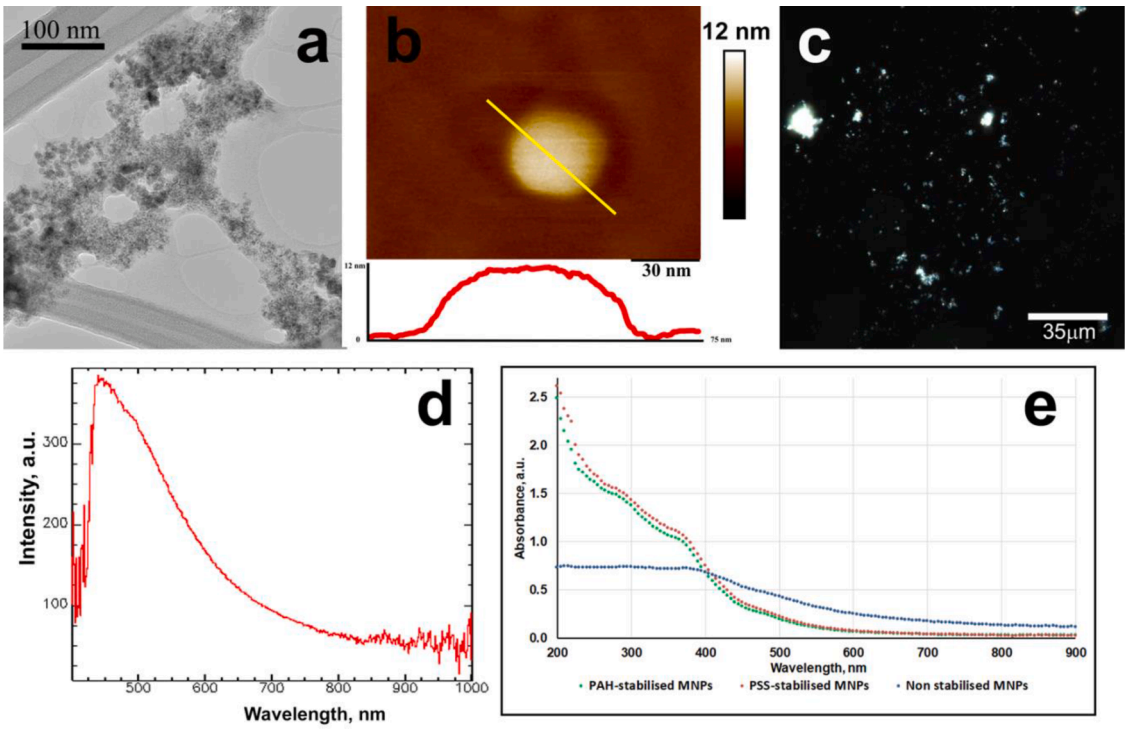

Fig. 2. Magnetic nanoparticles characterisation: a) TEM image of the as-synthesised iron oxide nanoparticles; b) AFM (height) image of the individual platelet-like nanoparticle along with the line profile; c) dark-field microscopy image of the suspended iron oxide nanoparticles; d) reflected light spectrum demonstrating the broad intensity peak at ca. 480 nm, e) optical absorbance of MNPs suspension in UV–vis waverange.

Dark-field microscopy and reflected light spectroscopy

Transmitted light dark-field (DF) optical microscopy imaging was performed as described elsewhere [17,18]. Briefly, DF images at high magnification (100 × lens) were collected using an Olympus BX51 upright microscope fitted with a CytoViva condenser. A fluorite Olympus objective with tunable numerical aperture was used for imaging and spectra collection. The reflected light spectra (within 400 – 1000 nm) were collected using a Specim spectrometer and Pixelfly USB (PCO) CCD camera, and then processed using ENVI 4.8 software. Alternatively, human hair samples were imaged in reflected light dark-field mode using a multiple focus stacking reconstruction followed by chemical hyperspectral mapping.

Results and discussion

Our strategy for rendering human hair with a uniform add-layer of biocompatible magnetic nanoparticles is summarized in Fig. 1. We synthesized iron oxide magnetic nanoparticles following our previously-published protocols, which resulted in fabrication of polyelectrolyte-coated MNPs having excellent adhesive properties to biological surfaces, such as microbial [16] cell walls or human cell membranes [19]. Hair, built essentially from keratin protein, to some extent resembles the biopolymer structure of microbial cell walls, therefore we theorised that the immersing of hair into aqueous suspensions of magnetic nanoparticles will result in modification of hair surfaces, similarly to the self-assembly of halloysite clay nanotubes reported in our previous studies [5,6]. Stimulated by practical considerations, we desired to

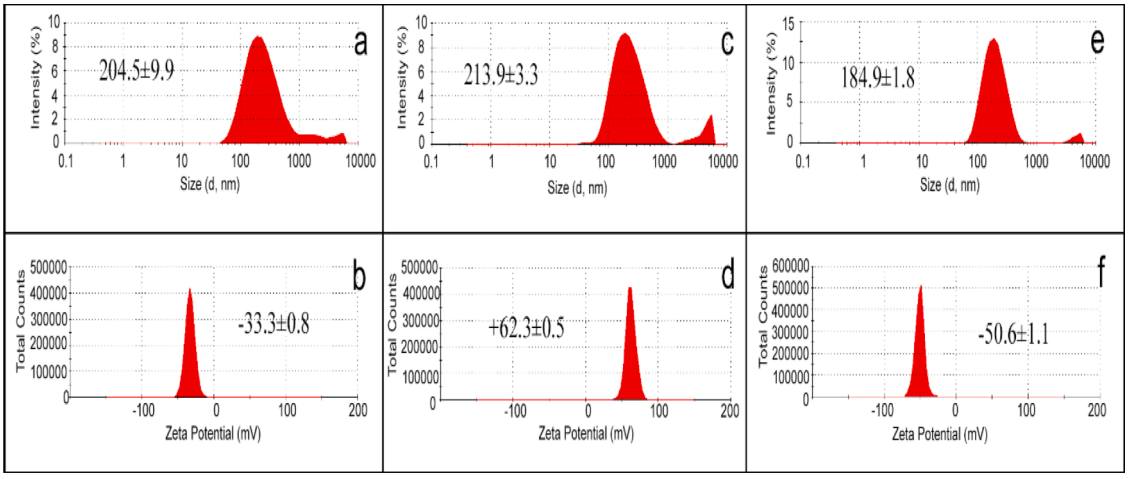

Fig. 3. Dynamic light scattering data demonstrating the hydrodynamic size distribution and electric zeta-potential of as-synthesised (a-b), PAH-stabilised (c-d), and PSS-stabilised (e-f) for iron oxide nanoparticles.

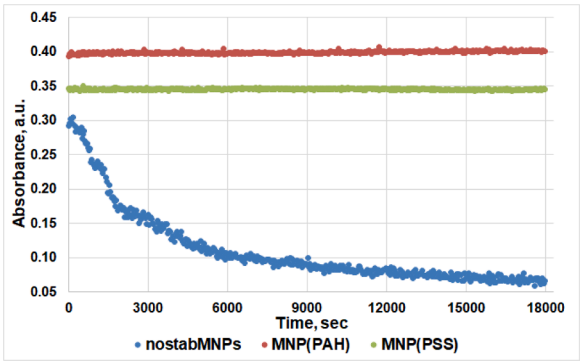

Fig. 4. Sedimentation stability of non-stabilised and polyelectrolyte-stabilised magnetic nanoparticles in water.

maintain all procedures as simple as possible, and resorted on fabrication of 20–30 nm iron oxide nanoparticles following the well-established co-precipitation protocol, with the subsequent stabilisation using either PAH or PSS polyelectrolytes, which allow for excellent colloid stability of the particles in a wide range of suspension pH and salt concentration [20]. These polyelectrolytes have been extensively studied as constituents for fabrication of layer-by-layer assembled surfaces and colloid particles, therefore we decided to focus on them for this study. Using these polyion stabilisation, we produced positive (+62 mV) or negative (−51 mV) magnetite of ca. 200 nm diameter allowing to optimise the coating taking into account the uneven hair surface charge distribution [7].

We characterised the nanoparticles obtained using advanced microscopy and spectroscopy techniques using TEM, AFM and dark-field optical microscopies (Fig. 2). The particles were relatively monodisperse, having spherical to platelet shapes and did not extensively aggregate in water even before stabilising with polyelectrolytes. The particles demonstrated effective light scattering with a broad reflection peak at 450 nm, which suggests that they will modify the optical properties of hair making them brown.

To further stabilise the MNPs, we coated them with either PAH or PSS, synthetic polyelectrolytes frequently used in fabrication of polymer microcapsules and for surface coatings [21,22]. The stabilised particles were investigated for surface charge and hydrodynamic diameter (Fig. 3), the results demonstrate that the deposition of polyelectrolytes, as expected, increase the surface potential (in the range 50–60 mV, positive in case of PAH, negative if PSS), while the hydrodynamic size was not considerably altered by the deposition of polyelectrolytes giving 200 ± 14 nm. The particle zeta-potential is above the colloidal stability threshold of 30 mV, and no aggregation was observed in polyelectrolytes-stabilised magnetite during dark-field microscopy experiments.

Colloid stability of particles for biomedical applications is an important factor for fabrication of long-lasting products, and requested time is months which well reachable with so high electric potential. We investigated the colloid stability of as-synthesised and polyelectrolytes-modified MNPs employing the sedimentation monitoring the optical absorption of aqueous suspension at 340 nm for 24 h. As demonstrated in Fig. 4, non-stabilised nanoparticles aggregated and settled within 2.5 h, whereas the polyelectrolytes-coated nanoparticles exhibited excellent colloid stability as tested up to one week.

Next, we applied the polyelectrolyte-stabilised nanoparticles to coat human hair, for this a 1 cm long human hair bundles (containing 5 −10 individual fibres) were immersed into the aqueous suspensions of PAH or PSS-stabilised MNPs (at 5 mg mL^{-1}) and incubated for 1 h under constant stirring. We imaged the nanoparticles deposition in real time in water using dark-field microscopy [23] (see Video 1 in Supplementary Information). It appears that the polyelectrolyte-stabilised magnetite attaches to the hair surface almost instantly upon immersion of hair shafts into nanoparticles suspensions. This correlates well with our previous studies where similar results were shown for the efficiency and speed of deposition of magnetic nanoparticles onto human and microbial cells [19,24]. Fig. 5 shows the distribution of PAH-coated MNPs on human hair in situ.

The formation of uniform layers of MNPs starting at the cuticle edges

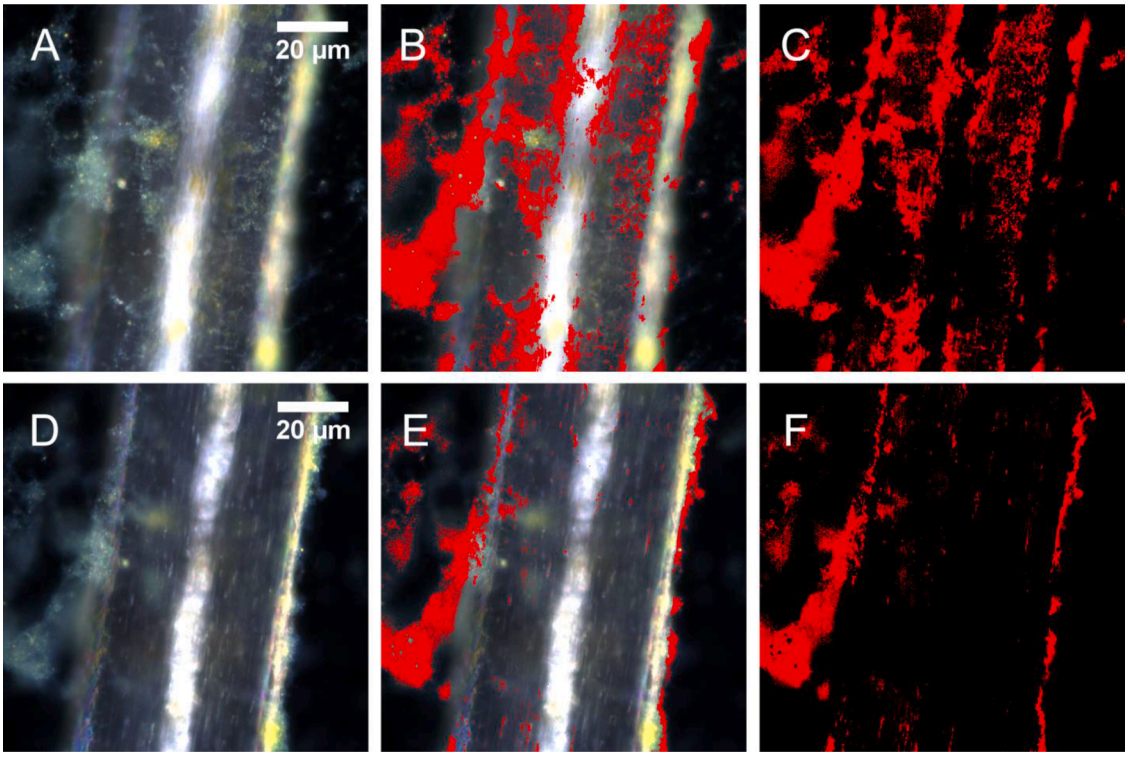

Fig. 5. Dark-field (a,d) and hyperspectral images (b-f) overlaid with PAH-stabilised magnetite distribution spectral maps obtained in water.

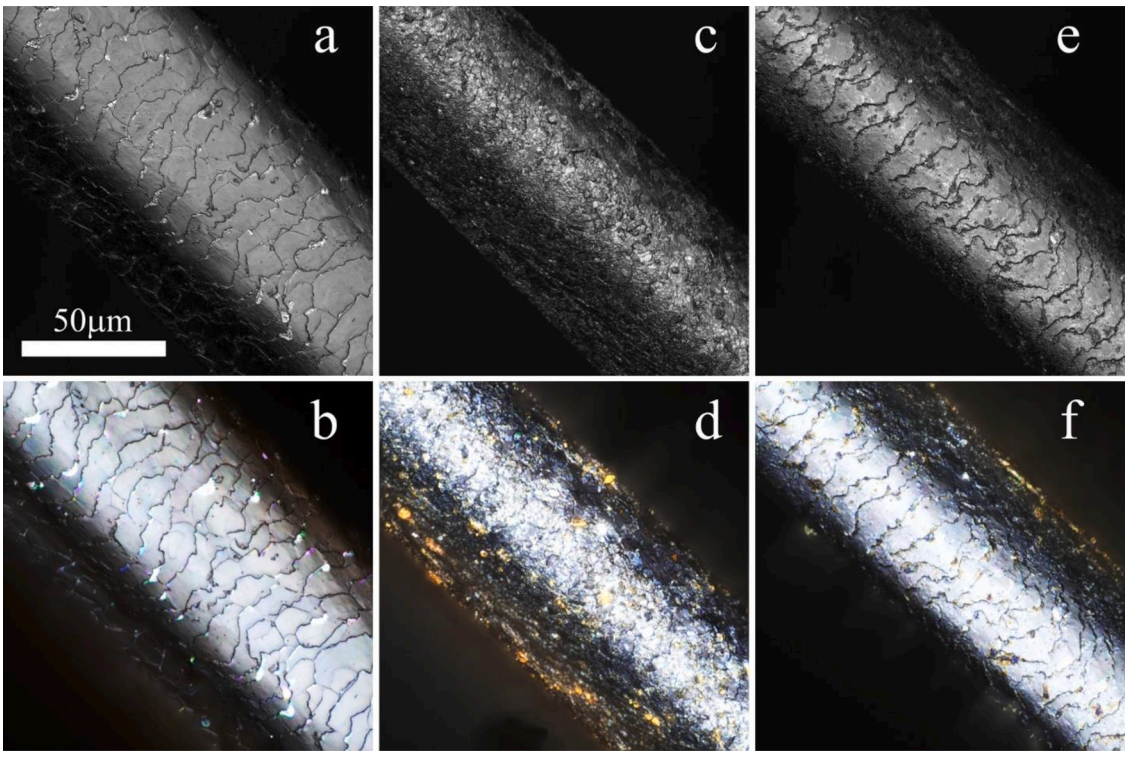

Fig. 6. Deposition of polyelectrolyte-stabilised magnetic nanoparticles alters the topography and colour of human hair. 3D confocal images demonstrating the fine structure of virgin human hair (a,b), human hair engineered with PAH-stabilised iron oxide nanoparticles (c,d) and human hair engineered with PSS-stabilised iron oxide nanoparticles (e,f). Top row – laser intensity monochrome images, bottom row – real colour optical images.

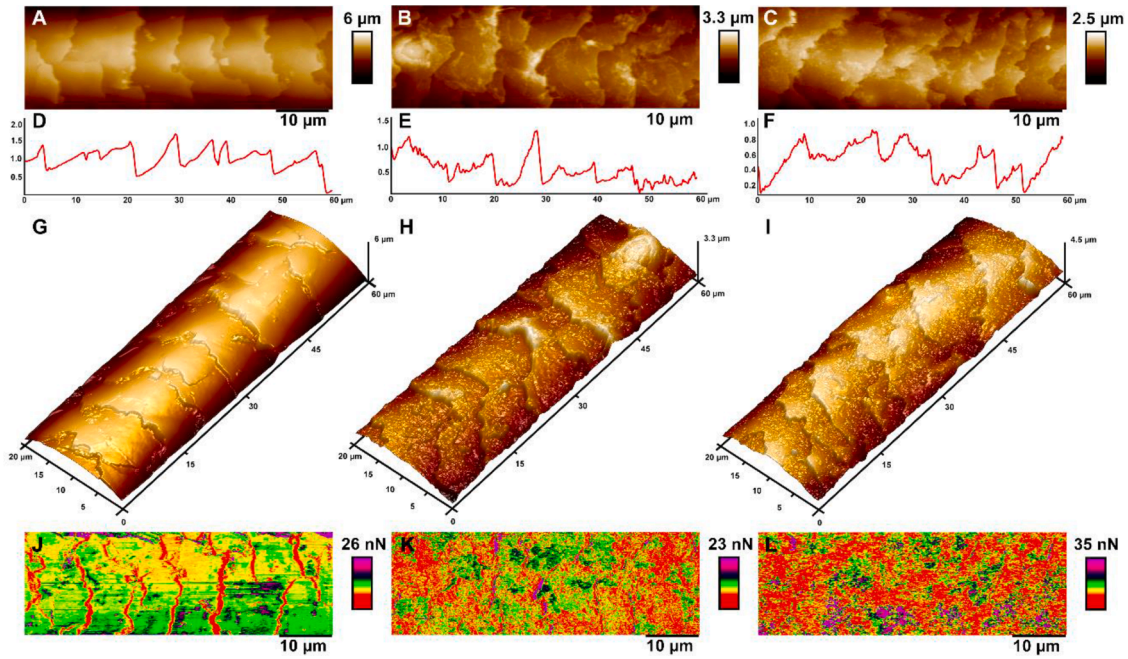

Fig. 7. Atomic force microscopy images of iron oxide nanoparticles-coated human hair surfaces. The virgin hair topography and non-specific adhesion images demonstrate the typical uniform distribution of cuticles, whereas the PAH-stabilised MNPs-coated and PSS-stabilised MNPs-coated hair images display the magnetic nanoparticles attached to cuticle surfaces and in the voids between the cuticles, altering the mechanical properties of the hair. Virgin hair: a,d,g,j; PAH-MNPs-coated hair: b,e,h,k; PSS-MNPs-coated hair: c,f,I,l.

and speeding further to full hair surface was further investigated in dried hair samples, as demonstrated in Figs. 6 and 7. The morphology of these layers was not similar for PAH and PSS modified magnetite. As shown in 3D laser intensity-based scanning confocal images (upper row in Fig. 6), PAH-coated MNPs produced the even coating of human hair, covering both the surfaces of the cuticles and the intercuticle voids, whereas PSS-coated MNPs were detected predominantly in the voids separating the individual cuticle area. This may be related to the map of the surface

Table 1
Microscale surface texture parameters[a] in pristine and nanoparticle engineered hair data.

Parameter	Virgin hair	PAH-MNPs/hair	PSS-MNPs/hair
Sq/μm	0.60 ± 0.07	1.27 ± 0.20	1.18 ± 0.14
Sa/μm	0.53 ± 0.09	1.10 ± 0.23	1.05 ± 0.16
Sz/μm	2.25 ± 0.37	4.91 ± 0.57	3.59 ± 0.57
Ssk	1.24 ± 0.14	1.37 ± 0.15	1.31 ± 0.13
Sku	2.07 ± 0.57	2.18 ± 0.56	1.96 ± 0.48
Sv/μm	0.66 ± 0.15	1.04 ± 0.69	0.63 ± 0.17
Sdq	1.31 ± 0.38	2.08 ± 0.55	1.88 ± 0.35
Sdr/%	31.3 ± 11	62.0 ± 19	52.2 ± 14

[a] Sq (root mean square height); Sa (arithmetical mean height); Sz (maximum height); Ssk (skewness); Sku (kurtosis); Sv (maximum pit depth); Sdq (root mean square gradient), Sdr (developed interfacial area ratio).

charge map, when all the hair surface is natively charged but the cuticle gaps are less charged [7] allowing for more magnetite accumulation. This is distinctly seen in the optical real-colour images (lower row in Fig. 6), where the characteristic brown colour of the iron oxide nanoparticles aggregates is demonstrated. The deposition of negatively-charged PSS-coated MNPs occurs in the same pattern as the self-assembly of negatively-charged halloysite nanotubes, demonstrated in our previous study [5,6,8], suggesting that hydrophobic interactions are responsible for the tailoring of likewise charged keratin cuticles and PSS-coated MNPs, the lipid coating of the voids surfaces being the primary target for MNPs deposition.

The numerical evaluation of hair surface roughness was performed by analysing data collected with a 3D laser scanning confocal microscopy and summarised in Table 1. Similarly to deposition of halloysite and sepiolite nanoclays [7,8], the deposition of magnetic nanoparticles onto hair surface resulted in the twofold increase of root mean square height, arithmetical mean height and maximum height of the hair surface features, which all indicate for a higher roughness. The positive skewness values were not changed significantly after the modification with both cationic and anionic MNPs, indicating the lower friction on the hair surface after the nanoparticle deposition. The kurtosis values below 3 suggest that the height distribution in both virgin and magnetic hair is skewed above the mean plane. These parameters indicate that the magnetic modification of hair does not significantly change the overall surface structure of hair. The increase in root mean square gradient and developed interfacial area ratio hybrid parameters suggest that the magnetic modification leads to the increase of hair surface area. Maximum pit height values are increased in hair specimens treated with PAH-coated MNPs, whereas in hair treated with PSS-coated MNPs this parameter remains similar to that of virgin hair, which is in agreement with predominant location of these nanoparticle in the cuticle gaps. Overall, the microscopic features of MNPs-coated hair resemble those of nanoclays-coated hair, indicating that the similar approaches can be used to modify hair with other colloidal particles.

Further, the patterns of deposition of MNPs on hair were investigated using surface characterisation with nanomechanical atomic force microscopy, AFM. The specimens were imaged in air, and the results are shown in Fig. 7. As one can see, the magnetised hair specimens demonstrate the random distribution of magnetic nanoparticles, regardless of their surface charge. The corresponding line profile data demonstrate the reduction of cuticle fluctuation intensity caused by deposition of MNPs. The nanomechanical maps confirm that the MNPs are distributed evenly, receding the non-specific adhesion between the hair surface and AFM tip.

This was surprising because we originally expected that the cationic PAH-modified MNPs will exhibit better affinity to negatively-charged hair surface. It has been shown previously that hair fibres are negatively charged [25], especially the cuticle edges [8], however, our results confirm that both cationic and anionic nanoparticles attach to the cuticles. These results can be explained by random charge distribution on hair surface facing the aqueous interface. Several previous studies [26,27] demonstrate that the negatively-charged areas are mostly associated with cysteine-residues rich areas of hair cuticles [26], predominantly located at the defected or broken edge areas. The surface charge distribution maps obtained using either scanning ion conductance microscopy [26] or electrostatic force microscopy [27] clearly show the coexistence of both positively and negatively-charged areas in human hair. However, the methods used are not capable to resolve the individual nanoparticles target sites. In this view, our results suggest that the electrostatic interactions are the main force driving the self-assembly of polyelectrolytes-stabilised MNPs, while the integral negative surface charge of hair fibres does not exclude a significant area fraction of the positive surface charge. Practically, this means that virtually any stabilising polymer can be used to facilitate the deposition

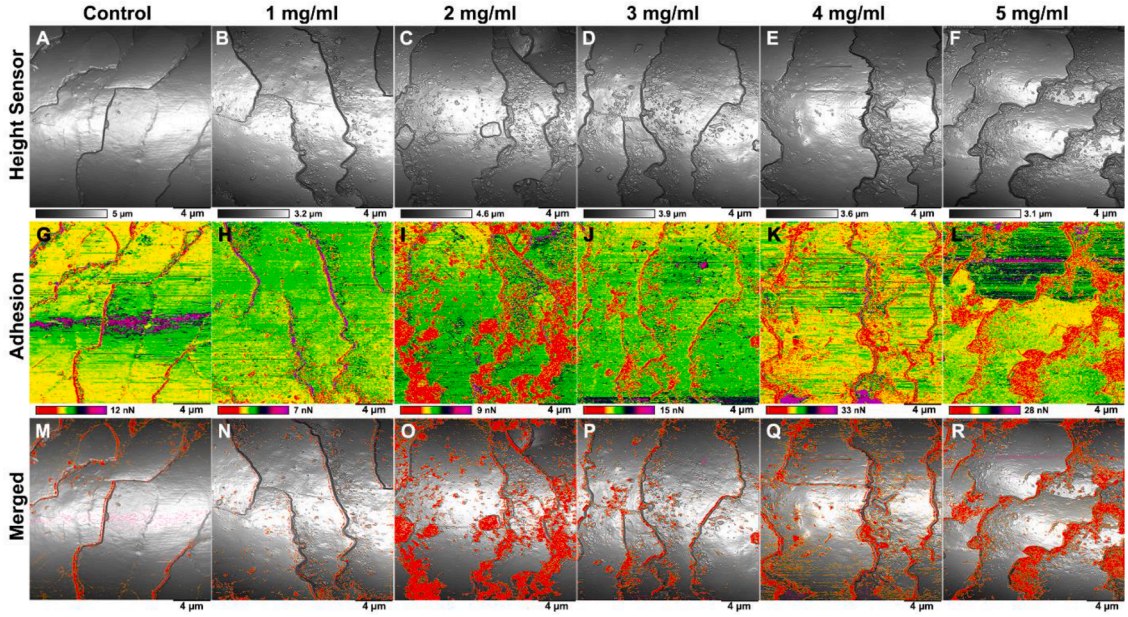

Fig. 8. AFM images of PSS-stabilised iron oxide nanoparticles-coated human hair surfaces at increasing concentrations. The virgin hair topography (top row) and, non-specific adhesion images (bottom row) demonstrate the effects of the colloidal particles concentration on coating density.

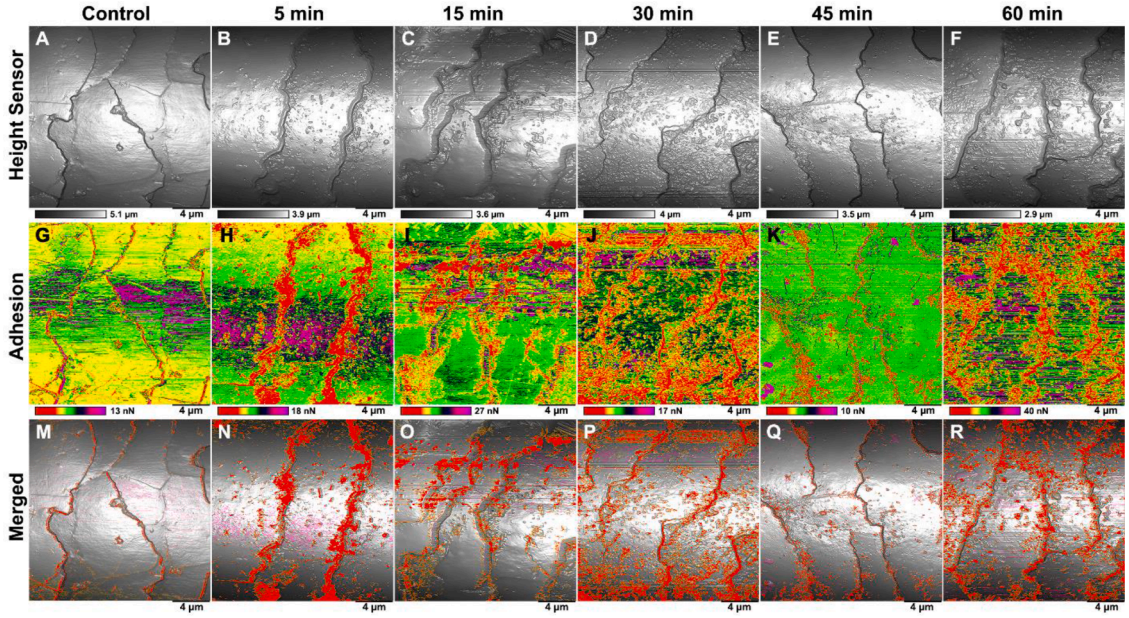

Fig. 9. AFM images of PSS-stabilised iron oxide nanoparticles-coated human hair surfaces at increasing incubation time. The virgin hair topography (top row) and, non-specific adhesion images (bottom row) demonstrate the effects of the colloidal particles deposition time.

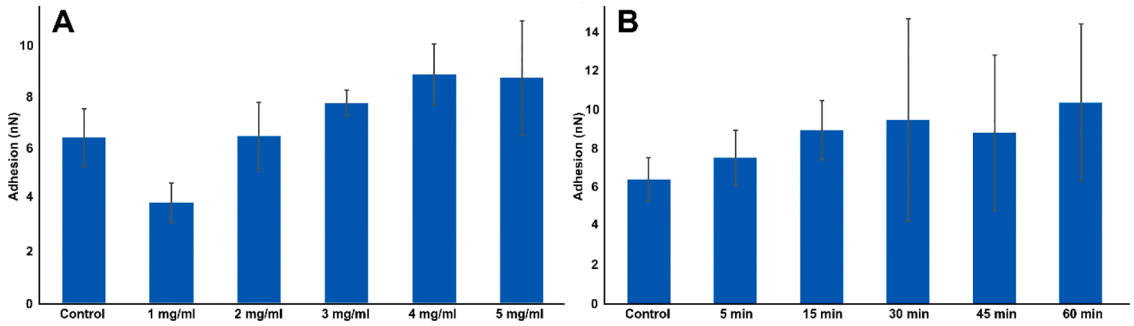

Fig. 10. The effects of PSS-coated MNPs concentration (a) and exposure time (b) on non-specific adhesion on hair surfaces measured as values per area.

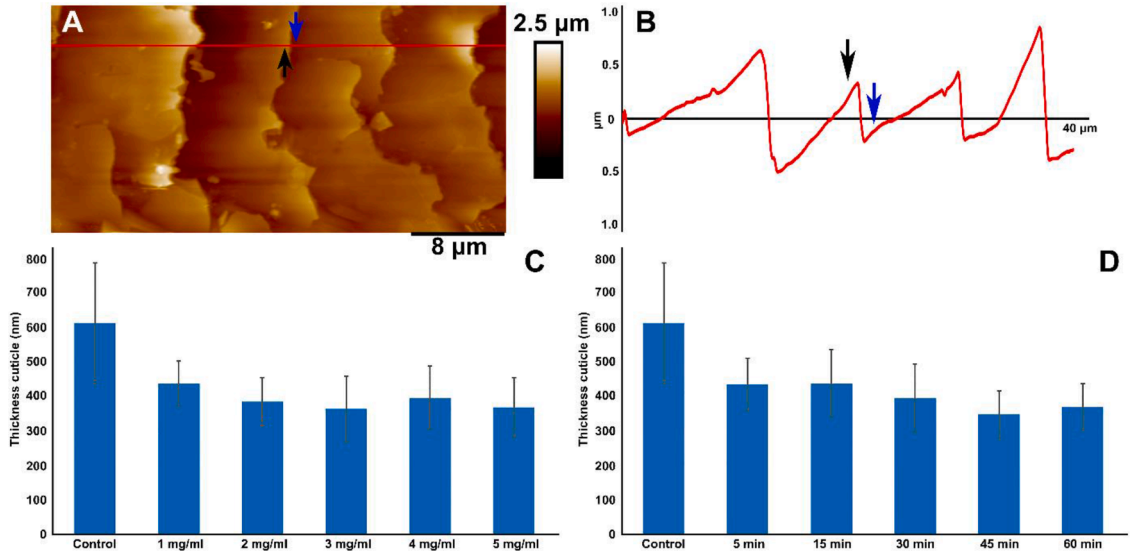

Fig. 11. Hair cuticles shown in AFM topography image (a) and the line profile (b); the resulting thickness values as function of coating concentrations (c) and exposure time (d).

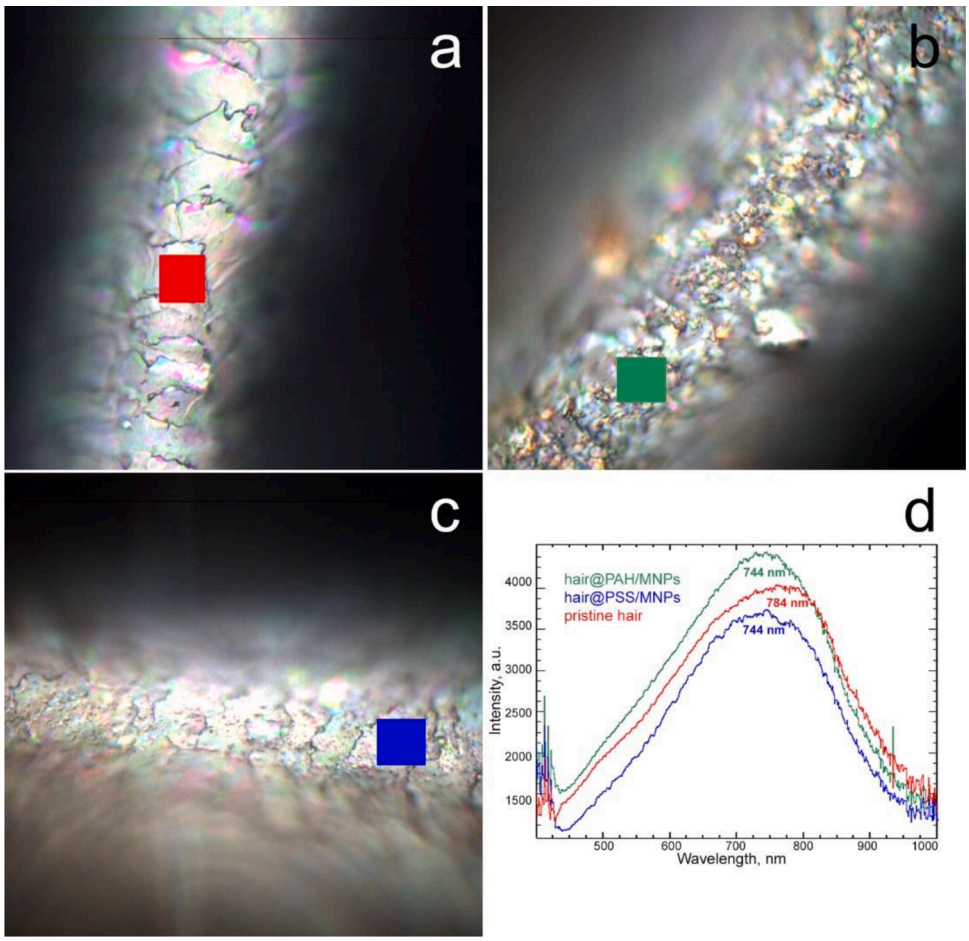

Fig. 12. Optical properties of virgin (a) and MNPs-coated hair studied by reflected light microscopy: PAH-MNPs (b) and PSS-coated MNPs (c); reflected light spectra of hair samples (d).

of MNPs onto hair surfaces. The main reason for using negatively-charged polyelectrolyte-coated nanoparticles was the fact that polycations, such as PAH, are still supposed to be toxic (due to complexation and disruption of cellular DNA). Although in our case the chances of PAH-coated NPs to get into the cytoplasm are very low, we opted for using a less toxic polymer. We therefore focused on PSS-coated nanoparticles, because they demonstrate lower toxicity than positively-charged polyelectrolytes [20] and provide more opportunities for covalent modification of PSS-tailored MNPs. We believe that virtually any polyelectrolyte can be used for this purpose, however in case of magnetite coated by either PAH or PSS there are equally important advantages, such as high surface potential, deposition speed, colloid stability and wide use in biomedical industry.

We investigated the effects of nanoparticles concentration and exposure time onto hair surface modification using AFM. Mapping the non-specific adhesion resulted in numerical non-specific adhesion data, indicating that 2 mg/mL is optimal and higher concentration does not significantly change in PSS-coated MNPs adsorption on hair (Fig. 8). As for the exposure time, it appears that the nanoparticles self-assemble on the hair within first 5 min of the exposure, and the prolonged incubation in suspension did not result in a more dense coating (Fig. 9), which corresponds well with real-time imaging using dark-field microscopy.

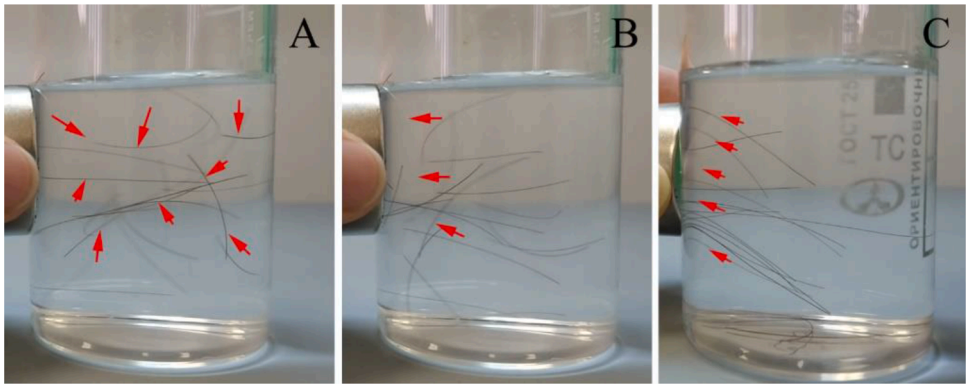

Fig. 13. Magnetic behaviour of PSS-coated MNPs-engineered human hair. Magnetic hair was first dispersed in pure water and agitated (a); then it was collected using a permanent magnet applied to the vessel after agitation (b and c).

Fig. 10 summarizes these data in mass per hair area coating, as well indicating as critical concentration and time 2 mg/ml and 5 min. PAH stabilized MNP coating data have shown a similar optimal concentration and deposition time.

Next, we investigated the structural and optical properties of magnetic hair obtained. We found that the deposition of PSS-coated MNPs resulted in ca. 40% reduction of hair cuticles thickens, suggesting that the nanoparticles fill gaps forming a uniform coating, regardless the exposure or concentration range, Fig. 11. This can be further exploited if one tailors drugs or dyes onto them, similarly to nanoclays, as we demonstrated earlier [28]. In case of magnetite nanoparticles, a wide selection of covalent and non-covalent surface modifications exist [29–31], thus making this approach a viable for hair surface engineering.

Apparently, the MNPs layer also affects the optical properties of hair surfaces. As shown in Fig. 12, the overall optical appearance of the coated hair becomes more glossy and reflective. In addition, a slight blue shift in reflectance spectra was detected. This suggests that mass hair coiffure might be optically modified as an alternative to traditional hair coloring.

Finally, as a proof of concept, we demonstrate qualitatively that deposition of MNPs onto human hair makes it magnetic, so that is using external magnetic field one can concentrate hair or spatially move it, Fig. 13.

Conclusion

We described a spontaneous coating of human hair with aqueous Fe_3O_4-nanoparticle colloids capable to tailor magnetic properties to hair, orienting and even moving them. 200 nm diameter magnetite particles modified by polyelectrolytes were successfully deposited in dense arrays, starting from cuticle gaps and spreading further over a major surface. These biocompatible and biodegradable magnetic nanoparticles may serve as carriers for drug loading and delivery for medical topical treatments. Under application of an external magnetic field, the nanoparticle magnetic ordering was obtained resulting in the hair alignment and attraction along the external field. We expect exploiting further cooperative phenomena on magnetized hair related with much needed in cosmetics hair volume control. Frizzy hair, also known as “mis-behaving” hair is a common problem for many people. With magnetic hair attraction, we can get the hair to behave better, with more alignment, and do not cause so much volume.

Funding

The work was funded by Russian Science Foundation grant 20–13–00,247.

Declaration of Competing Interest

The authors declare that they have no known competing financial interests or personal relationships that could have appeared to influence the work reported in this paper.

Acknowledgement

We thank Mr. Nikita Shkliar (Melytec LLC) for technical help with 3D confocal imaging.

Supplementary materials

Supplementary material associated with this article can be found, in the online version, at doi:10.1016/j.ceja.2022.100389.

References

[1] I. Guryanov, E. Naumenko, R. Fakhrullin, Hair surface engineering: combining nanoarchitectonics with hair topical and beauty formulations, Appl. Surf. Sci. Adv. 7 (2022), 100188, https://doi.org/10.1016/j.apsadv.2021.100188.
[2] S.Y. Han, E.K. Kang, I.S. Choi, Iron gall ink revisited: a surfactant-free emulsion technology for black hair-dyeing formulation, Cosmetics 8 (2021) 9, https://doi.org/10.3390/cosmetics8010009.
[3] S.Y. Han, S.-P. Hong, E.K. Kang, B.J. Kim, H. Lee, W. Kim, I.S. Choi, Iron gall ink revisited: natural formulation for black hair-dyeing, Cosmetics 6 (2019) 23, https://doi.org/10.3390/cosmetics6020023.
[4] K. Ariga, R. Fakhrullin, Materials nanoarchitectonics from atom to living cell: a method for everything, RSC Adv 95 (2022) 774–795, https://doi.org/10.1039/d1ra03424c.
[5] A. Panchal, G. Fakhrullina, R. Fakhrullin, Y. Lvov, Self-assembly of clay nanotubes on hair surface for medical and cosmetic formulations, Nanoscale 10 (2018) 18205–18216, https://doi.org/10.1039/C8NR05949G.
[6] G. Cavallaro, S. Milioto, S. Konnova, G. Fakhrullina, F. Akhatova, G. Lazzara, R. Fakhrullin, Y. Lvov, Halloysite/keratin nanocomposite for human hair photoprotection coating, ACS Appl. Mater. Interfaces 12 (2020) 24348–24362, https://doi.org/10.1021/acsami.0c05252.
[7] N. Rahman, A. Karan, Y. Lvov, Z. Liao, A. Parekh, R. Rughani, S. Muthukrishnan, Lawsone and indigo-loaded sepiolite nanofibers for hair coloring with sustained release, ACS Appl. Nano Mater. 5 (2) (2022) 1855–1863, https://doi.org/10.1021/acsanm.1c03472.
[8] N. Rahman, F.H. Scott, Y. Lvov, A. Stavitskaya, F. Akhatova, S. Konnova, G. Fakhrullina, R. Fakhrullin, Clay nanotube immobilization on animal hair for sustained anti-lice protection, Pharmaceutics 13 (9) (2021) 1477, https://doi.org/10.3390/pharmaceutics13091477.
[9] Y. Long, Y. Feng, Y. He, B. Luo, M. Liu, Hyaluronic acid modified halloysite nanotubes decorated with zif-8 nanoparticles as dual chemo- and photothermal anticancer agents, ACS Appl. Nano Mater. 5 (2022) 5813–5825, https://doi.org/10.1021/acsanm.2c01003.
[10] X. Cao, H. Liu, J. Cai, L. Chen, X. Yang, M. Liu, Chinese ink coated melamine foam with Joule heating and photothermal effect for strain sensor and seawater desalination, Compos. Part A: Appl. Sci. Manuf. 149 (2021), 106535, https://doi.org/10.1016/j.compositesa.2021.106535.
[11] A. Pankhurst, J. Connolly, S.K. Jones, J. Dobson, Topical review: applications of magnetic nanoparticles in biomedicine, J. Phys. D Appl. Phys. 36 (2003) R167–R181, https://doi.org/10.1088/0022-3727/36/13/201.
[12] V.E. Orel, M. Tselepi, T. Mitrelias, A. Rykhalskyi, A. Romanov, V.B. Orel, A. Shevchenko, A. Burlaka, S. Lukin, C.H.W. Barnes, Nanomagnetic modulation of tumor redox state, Nanomed.: Nanotechnol., Biol. Med. 14 (4) (2018) 1249–1256, https://doi.org/10.1016/j.nano.2018.03.002.
[13] S. Manju, K. Sreenivasan, Enhanced drug loading on magnetic nanoparticles by layer-by-layer assembly using drug conjugates: blood compatibility evaluation and targeted drug delivery in cancer cells, Langmuir 27 (2011) 14489–14496, https://doi.org/10.1021/la202470k.
[14] S. Mukherjee, L. Liang, O. Veiseh, Review recent advancements of magnetic nanomaterials in cancer therapy, Pharmaceutics 12 (2) (2020) 147, https://doi.org/10.3390/pharmaceutics12020147.
[15] R.T. Minullina, Y.N. Osin, D.G. Ishmuchametova, R.F. Fakhrullin, Interfacing multicellular organisms with polyelectrolyte shells and nanoparticles: a Caenorhabtidis elegans study, Langmuir 27 (12) (2011) 7708–7713, https://doi.org/10.1021/la2006869.
[16] S.A. Konnova, Y.M. Lvov, R.F. Fakhrullin, Nanoshell assembly for magnet-responsive oil-degrading bacteria, Langmuir 32 (47) (2016) 12552–12558, https://doi.org/10.1021/acs.langmuir.6b01743.
[17] S. Shaikhulova, G. Fakhrullina, L. Nigamatzyanova, F. Akhatova, R. Fakhrullin, Worms eat oil: Alcanivorax borkumensis hydrocarbonoclastic bacteria colonise Caenorhabditis elegans nematodes intestines as a first step towards oil spills zooremediation, Sci. Total Environ. 761 (2021), 143209, https://doi.org/10.1016/j.scitotenv.2020.143209.
[18] L. Nigamatzyanova, R. Fakhrullin, Dark-field hyperspectral microscopy for label-free microplastics and nanoplastics detection and identification in vivo: a Caenorhabditis elegans study, Environ. Pollut. 271 (2021), 116337, https://doi.org/10.1016/j.envpol.2020.116337.
[19] M.R. Dzamukova, E.A. Naumenko, E.V. Rozhina, A.A. Trifonov, R.F. Fakhrullin, Cell surface engineering with polyelectrolyte-stabilized magnetic nanoparticles: a facile approach for fabrication of artificial multicellular tissue-mimicking clusters, Nano Res. 8 (2015) 2515–2532, https://doi.org/10.1007/s12274-015-0759-1.
[20] E. Naumenko, F. Akhatova, E. Rozhina, R. Fakhrullin, Revisiting the cytotoxicity of cationic polyelectrolytes as a principal component in layer-by-layer assembly fabrication, Pharmaceutics 13 (8) (2021) 1230, https://doi.org/10.3390/pharmaceutics13081230.
[21] G.B. Sukhorukov, E. Donath, H. Lichtenfeld, E. Knippel, M. Knippel, A. Budde, H. Möhwald, Layer-by-layer self assembly of polyelectrolytes on colloidal particles, Colloids Surf. A: Physicochem. Eng. Aspects 137 (1998) 253–266, https://doi.org/10.1016/S0927-7757(98)00213-1.
[22] L. Van der Meeren, J. Verduijn, J. Li, E. Verwee, D.V. Krysko, B.V. Parakhonskiy, A. G. Skirtach, Encapsulation of cells in gold nanoparticle functionalized hybrid layer-by-layer (LbL) hybrid shells – remote effect of laser light, Appl. Surf. Sci. Adv. 5 (2021), 100111, https://doi.org/10.1016/j.apsadv.2021.100111.
[23] I.A. Iakovlev, A.Y. Deviatov, Y. Lvov, G. Fakhrullina, R.F. Fakhrullin, V. V. Mazurenko, Probing diffusive dynamics of natural tubule nanoclays with machine learning, ACS Nano (2022), https://doi.org/10.1021/acsnano.1c11025.

[24] J. García-Alonso, R.F. Fakhrullin, V.N. Paunov, Rapid and direct magnetization of GFP-reporter yeast for micro-screening systems, Biosens. Bioelectron. 25 (2010) 1816–1819, https://doi.org/10.1016/j.bios.2009.11.016.
[25] A.C. Lunn, R.E. Evans, The electrostatic properties of human hair, J. Soc. Cosmet. Chem. 28 (1977) 549–569.
[26] F.M. Maddar, D. Perry, R. Brooks, A. Page, P.R. Unwin, Nanoscale surface charge visualization of human hair, Anal. Chem. 91 (7) (2019) 4632–4639, https://doi.org/10.1021/acs.analchem.8b05977.
[27] V.M. Longo, V.F. Monteiro, A.S. Pinheiro, D. Terci, J.S. Vasconcelos, C. A. Paskocimas, E.R. Leite, E. Longo, J.A. Varela, Charge density alterations in human hair fibers: an investigation using electrostatic force microscopy, Int. J. Cosmet. Sci. 28 (2006) 95–101, https://doi.org/10.1111/j.1467-2494.2006.00280.x.
[28] A. Stavitskaya, S. Batasheva, V. Vinokurov, G. Fakhrullina, V. Sangarov, Y. Lvov, R. Fakhrullin, Antimicrobial applications of clay nanotube-based composites, Nanomaterials 9 (5) (2019) 708, https://doi.org/10.3390/nano9050708.
[29] H. Shagholani, S.M. Ghoreishi, M. Mousazadeh, Improvement of interaction between PVA and chitosan via magnetite nanoparticles for drug delivery application, Int. J. Biol. Macromol. 78 (2015) 130–136, https://doi.org/10.1016/j.ijbiomac.2015.02.042.
[30] M. Salem, Y. Xia, A. Allan, S. Rohani, E.R. Gillies, Curcumin-loaded, folic acid-functionalized magnetite particles for targeted drug delivery, RSC Adv 5 (2015) 37521–37532, https://doi.org/10.1039/C5RA01811K.
[31] M. Mohammadi, F.P. Aghaei, Magnetite Fe3O4 surface as an effective drug delivery system for cancer treatment drugs: density functional theory study, J. Biomol. Struct. Dyn. 39 (2020) 2798–2805, https://doi.org/10.1080/07391102.2020.1754915.